Asymmetry in Elementary Events of Magnetization Reversal in a Ferromagnetic/Antiferromagnetic Bilayer

V. I. Nikitenko,[1,2] V. S. Gornakov,[1,2] A. J. Shapiro,[1] R. D. Shull,[1] Kai Liu,[3] S. M. Zhou,[3] and C. L. Chien[3]

[1]*Metallurgy Division, National Institute of Standards and Technology, Gaithersburg, Maryland 20899*

[2]*Institute of Solid State Physics, Russian Academy of Sciences, Chernogolovka, Russia 142432*

[3]*Department of Physics and Astronomy, The Johns Hopkins University, Baltimore, Maryland 21218*

(Received 19 August 1999)

Real-time magneto-optical indicator film images reveal distinct asymmetry in the motion of a single domain wall in a wedged-NiFe/uniform-FeMn bilayer due to the nucleation and behavior of an exchange spring in the *antiferromagnetic layer.* Magnetization reversal from the ground state begins at the thick end of the wedge where the exchange anisotropy field (H_E) is minimal and the magnetostatic field (H_{MS}) is maximal, whereas reversal into the ground state begins from the thin end where H_E is maximal and H_{MS} is minimal.

PACS numbers: 75.70.Cn, 75.30.Et, 75.50.Kj

Domain wall (DW) nucleation and motion are among the most important phenomena in nonlinear physics, ranging from the reversal processes of magnetization in ferromagnets, polarization in ferroelectrics, to the magnetic and electric field response of superconductors. Domain walls are most prominently featured in ferromagnets, for which Landau and Lifshitz [1] proposed in 1935 an equation of magnetization dynamics and showed that the structure of a 180° DW is determined by the competition between the magnetocrystalline anisotropy (K) and exchange (A) energies. Within the wall width of $\delta = \pi\sqrt{A/K}$, the spins are twisted in a spiral creating a topologically stable exchange spring. In real ferromagnetic materials, the magnetization reversal proceeds by incoherent spin rotation, which causes DW nucleation in the regions with *maximal* magnetostatic field or crystal lattice defects [2].

In the last few years there has been a great deal of interest in studying the unique properties of magnetic nanostructures, involving small magnetic entities whose sizes are comparable to the DW width δ, in which there is a coexistence of ferromagnetic (FM) and antiferromagnetic (AF) exchange interactions [3–21]. One important class of nanostructures involves FM/AF bilayers [7–18], prominently featured in spin-valve field sensing devices with technological importance [19]. When a FM/AF bilayer is cooled in a magnetic field (H) to below the Néel temperature, a unidirectional (exchange) anisotropy is created [3]. This anisotropy is manifested by a shift of the hysteresis loop away from $H = 0$ by the amount of the exchange bias field H_E, and a significant increase in the coercive force (H_C) of the FM [3,15–18]. To date, the investigation of the microscopic magnetization reversal mechanisms in these systems has revealed drastic contradictions between theory and experiment in both the values of H_E and H_C.

It is now well recognized that the understanding of the exchange-biased FM/AF thin film lies in the peculiarities of nucleation and motion of domain walls of both the constituent FM and AF layers. However, detailed experimental study of the DW dynamics of the FM/AF bilayers has been severely hampered by the complicated multidomain structure, which occurs during switching, occurring within a narrow field range, from one single-domain state to another with an opposite magnetization.

Recently, macroscopic domain structures in an exchange-coupled bilayer of wedged-permalloy (Py = $Ni_{81}Fe_{19}$)/uniform-FeMn ($Fe_{50}Mn_{50}$) has been realized by exploiting the inverse dependence of the H_E on the FM layer thickness [16]. The magnetization switching process involves only *two macroscopic* domains separated by only *one* 180° DW, which moves along the wedge direction. Taking advantage of this unusually simple domain pattern, we have used the magneto-optical indicator film (MOIF) technique [17] to investigate the details of the DW nucleation and motion.

We have revealed in this work a distinct asymmetry of the DW motion in decreasing-field and increasing-field branches of a field cycle. We have observed direct experimental evidence that DW nucleation during the decreasing- and the increasing-field branches of the hysteresis loop proceeds at different locations of the FM layer. Contrary to that in free FM layers, the magnetostatic field stimulates DW formation in the exchange-coupled FM layer only in the decreasing-field branch. This distinct asymmetry in the elementary events of magnetization reversal is due to the local penetration of the exchange spring into, and its withdrawal from, the AF layer, proceeding on different hysteresis loop branches.

The sample used in this work has the structure of Py(110 Å–180 Å)/FeMn(300 Å)/Cu(300 Å)/Si and the dimension of 15 mm × 6 mm, with the long direction being the wedge direction. The film has an in-plane unidirectional anisotropy established by field cooling with the field applied perpendicular to the wedge direction. Magnetometry measurements and the MOIF imaging have been performed with the applied magnetic field H also perpendicular to the wedge. The MOIF imaging, which

measures the stray fields from the FM surface, has been used to map out the domains and the DW motion.

The hysteresis loop of the entire wedge sample measured at room temperature in a vibrating sample magnetometer is shown in Fig. 1(a) (the large scatter and slightly different values in M/M_s at saturation is probably due to the weak signal of a small sample). The corresponding domain patterns observed by MOIF are schematically shown in Fig. 1(b). Representative images taken at different stages during a hysteresis loop measurement are shown in Figs. [2–4]. The domain nucleation and DW motion can be divided into different stages for both the decreasing-field and increasing-field branches of a hysteresis loop.

In the decreasing-field branch [stages I–V in Fig. 1(b)], magnetization reversal from the fully magnetized state [stage I in Fig. 1(b)] occurs first at the two corner regions of the thick end of the wedged-FM [stage II in Fig. 1(b)], due to the presence of magnetic poles as in the free FM. Figure 2 shows the magnetization reversal in the lower right-hand corner of the thick end of the wedge. The MOIF technique detects the stray fields from a magnetic surface and nonuniform magnetization distribution inside the sample. Magnetic charges are revealed as dark and bright contrast on the gray background in slightly uncrossed polarizers, displaying the domains and the orientation of the magnetization within them. White arrows have been placed to show the magnetization direction. The sample in Fig. 2 was initially fully magnetized in a positive field of 14 mT, applied to the right [stage I in Fig. 1(b)]. As shown in Fig. 2(a), upon decreasing the field to −5.5 mT, small domains with opposite magnetization begin to appear, whereas the vast majority of the area is still magnetized to the right. When the external field continues to decrease, the domain with a reversed magnetization expands and encompasses the thick FM end [Figs. 2(b) and 2(c)], consolidating the small reversed domains in Fig. 2(a).

The corner domain evolution represented by Figs. 2(a)–2(c) also occurs at the lower left-hand corner of the thick end of the wedge, i.e., two corner domains develop simultaneously at the thick end of the FM [stage II in Fig. 1(b)]. Their continued growth in decreasing magnetic field leads to the joining of the two domains [stage III in Fig. 1(b)]. At this stage, the wedged FM consists of only two macroscopic domains with opposite magnetizations, separated by a 180° wall [16]. The resultant single DW is arc-shaped, bowing towards the thin end of the wedge.

The arc-shaped DW is driven towards the thin end of the wedge with further decrease of the magnetic field. Near the end of the magnetization reversal process, not two but only one domain is driven out of the sample in the middle section of the thin end of the wedge [stage IV in Fig. 1(b)]. This is clearly illustrated by examining the central region of the thin end as shown in Figs. 3(a)–3(c), where only one domain is driven out.

In the increasing-field branch of the hysteresis loop, from V to VIII [Fig. 1(b)], on a macroscopic level, the magnetization reversal seems to be just the stages of II to V in reverse. However, a closer examination shows crucial

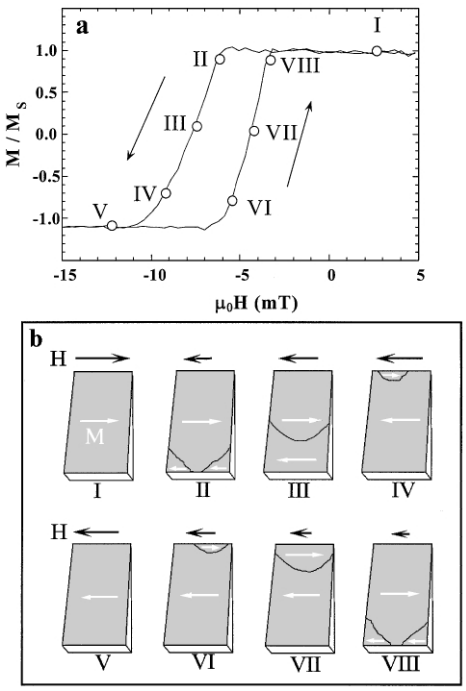

FIG. 1. Hysteresis loop (a) and schematics (b) of domain structure at the different stages (I–VIII) of magnetization reversal of a wedged NiFe/uniform FeMn bilayer.

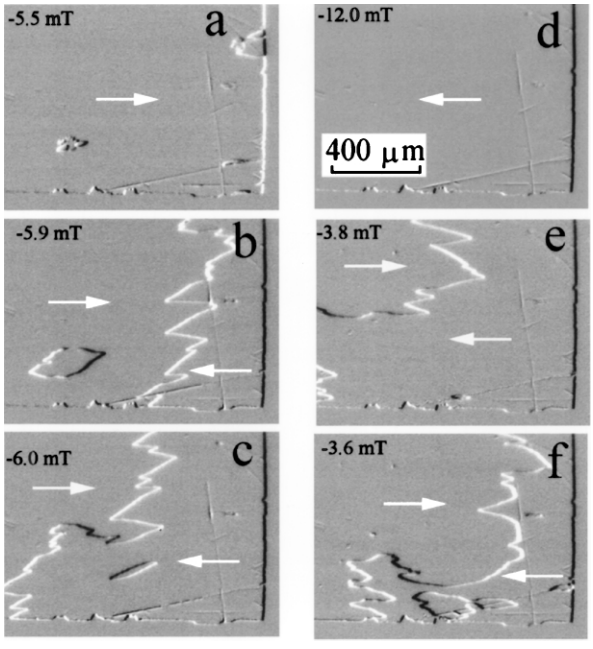

FIG. 2. MOIF images of domain structure at the lower right-hand corner of the thick end of the wedge at various points of the hysteresis loop corresponding to stages II (a)–(c) and VIII (d)–(f) in Fig. 1. The white arrows indicate the direction of magnetization.

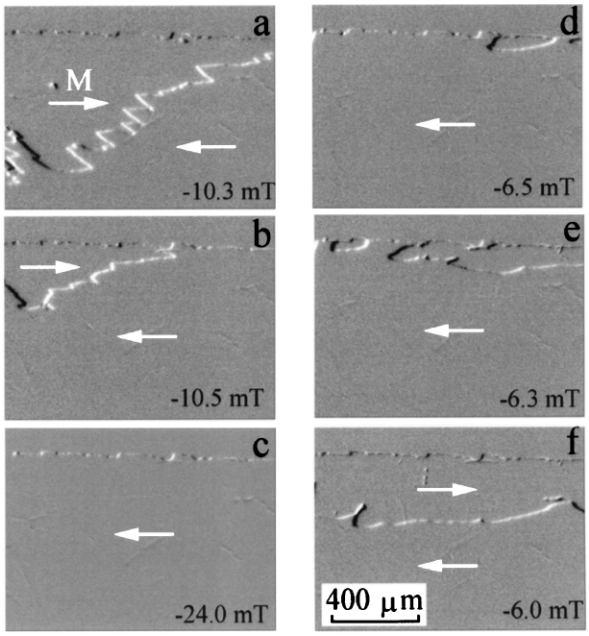

FIG. 3. MOIF images of domain structure in the center of the thin end of the wedge at various points of the hysteresis loop corresponding to stages IV (a)–(c) and VI (d)–(f) in Fig. 1. The white arrows indicate the direction of magnetization.

differences between the increasing-field and decreasing-field branches due to unusual DW nucleation features and the asymmetry in the DW motion. The magnetization reversal process starts from a saturated magnetization pointing to the left [Fig. 3(c) and stage V in Fig. 1(b)]. As the field is increased to -6.6 mT, initial nucleation of the reversal domain occurs in the middle part of the thin end [Fig. 3(d)], but at a *different* location from the one that the domain disappeared during the decreasing-field branch of the loop [Fig. 3(b)]. As the magnetic field further increases, the newly reversed domains with magnetization pointing to the right extend along the thin end of the wedge to form a continuous domain. At the same time, the DW moves towards the thick end of the wedge [Figs. 3(e) and 3(f), stage VI in Fig. 1(b)]. Both the domain shape and DW dynamics differ from those observed during the decreasing-field branch. The DW is zigzag in shape in the field-decreasing process, is more mobile, and has a large propensity to creep [Fig. 3(a)]. In the field-increasing process, the DW is much more rounded in shape, indicating a different distribution of the localized magnetostatic charges.

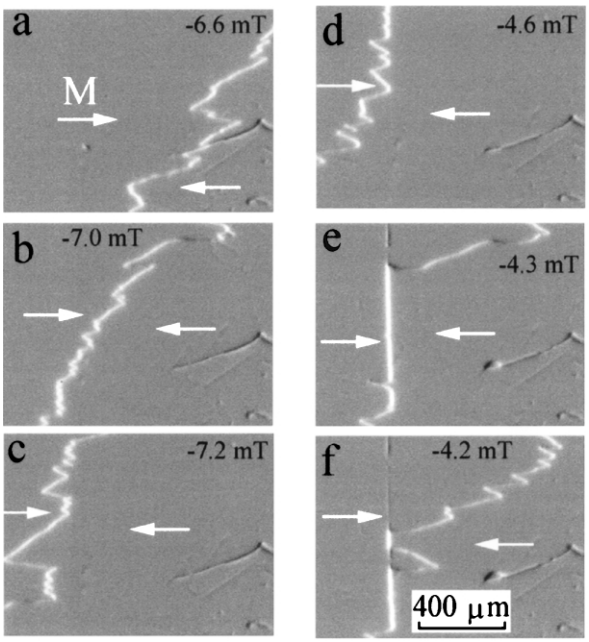

FIG. 4. MOIF images of domain wall moving in opposite directions at stages III (a)–(c) and VII (d)–(f) of the hysteresis loop in Fig. 1. The white arrows indicate the direction of magnetization.

As the field is further increased, the DW moves towards the thick end of the wedge, also arc-shaped as before, except that the central part of the DW is the leading one [stage VII in Fig. 1(b)]. When this central part of the macroscopic DW reaches the thick end of the wedge, two corner domains remain in the sample as shown in Figs. 2(d)–2(f) [stage VIII in Fig. 1(b)]. Eventually DW's of these two domains are driven out of the wedge corners [Figs. 2(d)–2(f)], and the sample returns to the fully magnetized ground state shown in stage I of Fig. 1(b).

In stages III and VII of Fig. 1(b) there is an arc-shaped DW. The central part of the DW is perpendicular to the wedge direction, but with larger curvature at both ends of the DW. This is illustrated in Fig. 4, showing the motion of the curved DW near the sample edge. Comparing the domain pattern of the same region for the decreasing [Figs. 4(a)–4(c)] and increasing branches [Figs. 4(d)–4(f)], one immediately notices a pronounced asymmetry in the DW-pinning site interactions. In the increasing-field branch, the DW is strongly pinned by a rectilinear crystal defect, whereas in the decreasing-field branch this defect does *not* influence the DW motion.

The key observation revealed by the MOIF images is the acute *asymmetry* in the DW nucleation, its motion, and its interactions with crystal lattice defects. It has been revealed in every region of the sample as shown in Figs. 2–4. This asymmetry in the DW behavior is unique to exchange-coupled AF/FM bilayers. In either a single FM layer or a single AF layer, such asymmetry *does not* exist. As described below, the observed asymmetry in FM/AF bilayers reveals the presence of an AF domain wall, which has also been indicated by more recent micromagnetic models.

In the first model of exchange coupling of FM/AF bilayers, the AF layer was assumed to have a static spin structure with an uncompensated interfacial spin structure [3]. During switching of the exchange-coupled FM layer, the spin structure of the AF layer remains unchanged. Such models with a static AF spin structure could *not* explain asymmetry in the DW motion. The pinning centers for the DW would be the

same for both increasing-field and decreasing-field branches, such as those encountered in a free FM layer. The observed asymmetry is incompatible with models having a static AF spin structure.

A number of subsequent models of FM/AF exchange coupling have concluded the existence of DWs in the AF [7,8,11,17,18]. When the magnetization is reversed by an external field, the AF moments at the interface will be rotated with the FM moments, with spiraling AF moments below the interface, similar to that of the exchange spring in a DW of a ferromagnet [1] or in the exchange-spring magnets [20,21]. While direct observation of such a specific exchange spring in the AF layer has not been possible, the asymmetry of the DW behavior in the FM layer revealed here gives strong, albeit indirect, evidence of the formation of the proposed spin structure during bilayer magnetization reversal. However, even the recent models [7,11,14] did not take into account the inhomogeneity of magnetization reversal processes of the FM layer. As described below, our results indicate the formation of a new type of *hybrid* AF/FM domain wall.

During the magnetization reversal process, the nucleation and motion of the hybrid DW involve twisting and untwisting of the spins in both the FM and AF layers. In the decreasing-field branch of the hysteresis loop, the DW nucleation begins in the thick parts of the FM layer (Fig. 2), where the exchange field H_E is minimal. In this case, the magnetostatic field increases the force exerted by the external field on the FM spins and thus on the ferromagnetic part of the hybrid DW. At higher magnetic fields, the exchange spring overcomes the pinning sites in the FM and penetrates into the AF layer. Therefore, DW formation in the FM initiates at the locations with both minimal H_E (thick end of the wedge) and maximal H_{MS} (the two corners at the thick end).

In the increasing-field branch of the hysteresis loop, magnetization reversal begins in the thin region of the sample where H_E is maximal. The large magnitude of the interface exchange field initiates the untwisting of the exchange spring. Since the untwisting occurs first at places with the largest anisotropy energy inside the AF layer, it is not necessary to nucleate the DW in both the FM and AF layers. Rather, the DW in the AF now moves towards and penetrates into the FM and nucleates new domains with the ground state magnetization. Further untwisting of the exchange spring gives rise to motion of the hybrid AF/FM DW toward the thick end of the wedge. The magnetostatic field in the increasing-field branch of the hysteresis loop acts against the untwisting of the exchange spring. Therefore, DW formation in a FM initiates at sample locations with both maximal H_E and minimal H_{MS} (center of thin end).

The observed asymmetry of the DW motion shown in Fig. 4 is another manifestation of the antiferromagnetic DW, which is sensitive to local anisotropy changes caused by crystal defects in the AF layer. If a defect is to decrease (increase) the local crystalline anisotropy, the energy associated with the spin twisting decreases (increases). During the untwisting process, the AF spins, and consequently the FM spins, will rotate less readily (more easily), leading to pinned (unhindered) DW motion.

In summary, we have directly observed macroscopic domain structures in a wedged-Py/uniform-FeMn exchange-coupled bilayer with the anisotropy direction perpendicular to the wedge direction. Magnetization reversal from a fully magnetized state starts at the thick corners of the wedge where the exchange energy is minimal and the magnetostatic energy is maximal. The two edge domains then join and form a macroscopic reversal domain, separated from the original domain by a 180° macroscopic DW. The DW propagates toward and eventually vanishes at the thin end of the wedge where the exchange energy is maximal and the magnetostatic energy is minimal. The observed asymmetry in the DW motion, incompatible with a static AF spin structure, indicates the presence of a mobile DW (exchange spring) in the antiferromagnet.

Work at JHU was supported by NSF Grant No. DMR96-32526.

[1] L. D. Landau and E. M. Lifshitz, Phys. Z. Sowjetunion **8**, 153 (1935).
[2] See, e.g., W. F. Brown, Jr., *Micromagnetics* (Interscience, New York, 1963).
[3] W. H. Meiklejohn and C. P. Bean, Phys. Rev. **102**, 1413 (1956); **105**, 904 (1957).
[4] P. Grünberg *et al.*, Phys. Rev. Lett. **57**, 2442 (1986).
[5] S. S. P. Parkin, N. More, and K. P. Roche, Phys. Rev. Lett. **64**, 2304 (1990).
[6] J. Unguris, R. J. Celota, and D. T. Pierce, Phys. Rev. Lett. **67**, 140 (1991).
[7] D. Mauri *et al.*, J. Appl. Phys. **62**, 3047 (1987).
[8] A. P. Malozemoff, Phys. Rev. B **35**, 3679 (1987); J. Appl. Phys. **63**, 3874 (1988).
[9] A. Berger and H. Hopster, Phys. Rev. Lett. **73**, 193 (1994).
[10] J. Nogues *et al.*, Phys. Rev. Lett. **76**, 4624 (1996).
[11] N. C. Koon, Phys. Rev. Lett. **78**, 4865 (1997).
[12] N. J. Gökemeijer, T. Ambrose, and C. L. Chien, Phys. Rev. Lett. **79**, 4270 (1997).
[13] K. Takano *et al.*, Phys. Rev. Lett. **79**, 1130 (1997).
[14] T. C. Schulthess and W. H. Butler, Phys. Rev. Lett. **81**, 4516 (1998).
[15] D. V. Dimitrov *et al.*, Phys. Rev. B **58**, 12 090 (1998).
[16] S. M. Zhou, Kai Liu, and C. L. Chien, Phys. Rev. B **58**, R14 717 (1998).
[17] V. I. Nikitenko *et al.*, Phys. Rev. B **57**, R8111 (1998).
[18] M. D. Stiles and R. D. McMichael, Phys. Rev. B **59**, 3722 (1999).
[19] B. Dieny *et al.*, Phys. Rev. B **43**, 1297 (1991).
[20] Eckhart F. Kneller and Reinhard Hawig, IEEE Trans. Magn. **27**, 3588 (1991).
[21] E. Fullerton *et al.*, Phys. Rev. B **58**, 12 193 (1998).